

Gravitational lensing by wormholes

Tushar Kanti Dey¹ and Surajit Sen²

Department of Physics

Guru Charan College

Silchar 788004, India

Abstract

We have investigated the gravitational lensing by two wormholes, viz., Janis - Newman-Winnicour (JNW) wormhole and Ellis wormhole. The deflection angle in the strong field limit is calculated and various lens parameters of two wormholes are compared. It is shown that the JNW wormhole exhibits the relativistic images, while the Ellis wormhole does not have any relativistic images due to the absence of its photon sphere.

Keywords: gravitational lensing, wormhole

PACS No. 4.40 -b, 95.30 Sf, 98.62 Sb

¹tkdey54@rediffmail.com

²ssen55@yahoo.com

I. Introduction

The gravitational lensing (GL) is regarded as one of the most effective tool of probing a number of interesting phenomena of the universe. Some of these phenomena charted recently are the existence of various interesting astrophysical objects e.g., black holes, super-dense neutron stars, exotic matter, wormholes, naked singularity etc and the detection of these objects may eventually en route to the possible connection between the quantum theory and gravity. Since the classic observation of the bending of light in 1919, the general theory of relativity passes a number of stringent tests mainly in the weak gravitational field limit. Out of these tests, the observation of Einstein ring and the double or multiple mirror images is the most profound example GL effect [1, 2, 3]. This success leads to explore other extreme regime, namely, the GL effect in the strong gravitational field limit, where the relativistic images with a separation of the order of a few micro-arcseconds has been predicted [4 - 7]. Out of various intriguing objects mentioned above, recently the wormhole has renewed wide attention because of its own right. Originally proposed by Morris and Thorne in 1988 [8], the existence of this wormhole cannot be ruled out by the general theory of relativity, although its feasibility requires the existence of the exotic matter [8 - 10]. Therefore it is interesting to study the GL effect caused by the wormhole particularly in the strong gravitational field which is essentially related with other important issues such as the evidence of the exotic matter, formation of caustic etc [11, 12].

The GL effect, either in the weak or strong gravitational field, primarily involves the solution of the null geodesic equation. Its solution in terms of the angle of deflection of light can be expressed by the integral [13]

$$\hat{\alpha}(r_0) = 2 \int_{r_0}^{\infty} \sqrt{A(r)/D(r)} \sqrt{\left[\left(\frac{r}{r_0} \right)^2 \frac{D(r)}{D(r_0)} \frac{B(r_0)}{B(r)} - 1 \right]^{-1}} \frac{dr}{r} - \pi, \quad (1)$$

where $A(r)$, $B(r)$ and $D(r)$ be coefficient of the space-space, time-time and angular parts of the generic line element which reduce to unity in the asymptotic limit of r and r_0 be the distance of closest approach of light to the compact object which causes the lensing effect. It follows from the simple geometry that the above integral in Eq.(1) is related to the basic

lens parameters as [4, 5]

$$\tan\beta = \tan\theta - \alpha(r_0), \quad (2)$$

where,

$$\alpha(r_0) = \frac{D_{ds}}{D_s} [\tan\theta + \tan(\hat{\alpha}(r_0) - \theta)]. \quad (3)$$

Here β and θ be the source and the image position measured from the optic axis, D_{ds} and D_s be the source-lens and source-observer distance respectively. The total magnification of a circularly symmetric GL is given by [5]

$$\mu = \left(\frac{\sin\beta}{\sin\theta} \frac{d\beta}{d\theta} \right)^{-1} \quad (4)$$

and the tangential and radial magnification are given by

$$\mu_t = \left(\frac{\sin\beta}{\sin\theta} \right)^{-1}, \quad \mu_r = \left(\frac{d\beta}{d\theta} \right)^{-1}. \quad (5)$$

Thus calculation of various lens parameters amounts to the evaluation of the bending angle given by Eq.(1). In the recent past several attempts have been made to calculate the elliptical integral mainly by Virbhadra and Ellis [4, 5], Virbhadra, Narasimha and Chitre [6], Bozza [7], Nandi et al [9], Amore and Diaz [14] and others [15]. Out of these approaches recently Amore and Diaz (AD) have proposed an elegant method to calculate the deflection angle even in the strong gravitational field limit [14]. Their method relies primarily on two approximations: firstly, they have used the linear delta function technique to approximate the above integral with a ansatz potential and then, secondly, they use the principle of minimal sensitivity (PMS) to minimize the parametric dependence to the deflection angle in the strong field limit. The primary objective of the present work is to study the GL effect caused due to the Janis-Newman-Winnicour (JNW) [5, 9, 10, 16, 17] and Ellis wormhole [8, 18] in the strong gravitational field using the methodology developed by AD.

The remaining Sections of the paper are organized as follows: in Section-II we review the essence of the approach of AD to develop the general formalism of solving Eq.(1) in the strong gravitational field. Section-III discusses the explicit calculation of the bending angle in the strong and weak field limit for these wormholes. In Section-IV we compare basic features of two wormholes and discuss their magnifications. We conclude by summarizing the main results in Section V and discuss the outlook.

II. Formalism

To find out the deflection angle following the procedure outlined by Amore and Diaz [14], we change the variable $r = r_0/z$ and define the potential function

$$V(z) = z^2 \frac{D(r_0/z)}{A(r_0/z)} - \frac{D^2(r_0/z)B(r_0)}{A(r_0/z)B(r_0/z)D(r_0)} + \frac{B(r_0)}{D(r_0)}. \quad (6)$$

Using Eq.(6), the Eq (1) can be expressed as

$$\hat{\alpha}(r_0) = 2 \int_0^1 \frac{dz}{\sqrt{V(1) - V(z)}} - \pi. \quad (7)$$

To evaluate the integral in Eq.(7) AD have used the linear delta shifted potential as

$$V_\delta(z) = V_0(z) + \delta(V(z) - V_0(z)), \quad (8)$$

where $V_0(z) = \lambda z^2$ be the ansatz potential. The potential in Eq.(6) can be expressed as

$$V(z) = \sum_{n=1}^{\infty} v_n z^n, \quad (9)$$

where v_n be the coefficient of z which are to be determined. Plucking back Eq.(9) into Eq.(7) a straight forward algebra gives the deflection angle to be

$$\hat{\alpha}^1(r_0) = \frac{3\pi}{2\sqrt{\lambda}} - \frac{1}{\lambda^{3/2}} \sum_{n=1}^{\infty} v_n \Omega_n - \pi, \quad (10)$$

where the superscript 1 corresponds to the first order expansion of the integrand in Eq.(7) and Ω_n is given by

$$\Omega_n = \sqrt{\pi} \frac{\Gamma(n/2 + 1/2)}{\Gamma(n/2)}. \quad (11)$$

In Eq.(10), the unknown parameter λ is obtained by the PMS,

$$\left. \frac{\partial \hat{\alpha}^1}{\partial \lambda} \right|_{\lambda=\lambda_{PMS}} = 0, \quad (12)$$

and the expression of the PMS approximated deflection angle is given by

$$\hat{\alpha}_{PMS}^1(r_0) = \pi \left[\sqrt{\frac{\pi}{2\rho}} - 1 \right], \quad (13)$$

where

$$\rho = \sum_{n=1}^{\infty} v_n \Omega_n, \quad (14)$$

be the transformed potential which needs to be calculated for the metric in consideration. Eq.(13) is the form of the deflection angle which was originally derived by AD and in next Section we proceed to calculate it for two distinct wormhole configurations.

III. Calculation of deflection angle due to wormholes

a) Janis-Newman-Winnicour wormhole

The matter with non-vanishing exotic scalar charge is described by the Janis-Newman-Winnicour (JNW) metric

$$ds^2 = \left(1 - \frac{2m}{r}\right)^\gamma dt^2 - \left(1 - \frac{2m}{r}\right)^{-\gamma} dr^2 - r^2 \left(1 - \frac{2m}{r}\right)^{1-\gamma} (d\theta^2 + \sin^2 \theta d\phi^2), \quad (15)$$

where $\gamma = \frac{M}{m}$ with M be the Arnowitt, Deser and Misner (ADM) mass related to the asymptotic scalar charge $q \left(= m\sqrt{\frac{2(1-\gamma^2)}{\kappa}}\right)$ by $M^2 = m^2 - \frac{1}{2}\kappa q^2$. For the EMS (Einstein Massless Scalar) theory, the solution of the covariant scalar solution $\Phi(r)$ is related with the ADM mass by $\Phi(r) = \sqrt{\frac{1-\gamma^2}{2\kappa}} \ell n\left[1 - \frac{2m}{r}\right]$ where $\kappa (> 0)$ represents the matter-scalar field coupling constant. Several authors have calculated the deflection angle for $\gamma \leq 1$ with the scalar charge is real [6, 7], however for $\gamma > 1$, which corresponds to the JNW wormhole, the scalar charge is a complex quantity [9, 10].

The potential function $V(z)$ in Eq.(6) can be easily read off for the JNW metric as

$$V(z) = z^2 \left(1 - \frac{2mz}{r_0}\right) - \left(1 - \frac{2mz}{r_0}\right)^{2(1-\gamma)} \left(1 - \frac{2m}{r_0}\right)^{2\gamma-1} + \left(1 - \frac{2m}{r_0}\right)^{2\gamma-1} \quad (16)$$

and it can be expanded around $z = 0$ to give

$$V(z) \approx v_1 z + v_2 z^2 + v_3 z^3 + O(z^4), \quad (17)$$

where

$$v_1 = \frac{4m}{r_0} \left(1 - \frac{2m}{r_0}\right)^{2\gamma-1} (1 - \gamma), \quad (18)$$

$$v_2 = 1 - \frac{4m^2}{r_0^2} \left(1 - \frac{2m}{r_0}\right)^{2\gamma-1} (1-\gamma)(1-2\gamma), \quad (19)$$

$$v_3 = -\frac{2m}{r_0} - \frac{16m^3}{3r_0^3} \left(1 - \frac{2m}{r_0}\right)^{2\gamma-1} \gamma(1-\gamma)(1-2\gamma), \quad (20)$$

respectively. Using Eqs.(11) and (17), the transformation potential ρ can be easily read off from Eq.(14) and the PMS approximated deflection angle in Eq.(13) is given by (for convenience, we have dropped the superscript 1 and the subscript PMS.)

$$\hat{\alpha}(r_0) = \pi \left[\sqrt{\frac{3\pi(r_0 - b)r_0^2}{3r_0(r_0 - b)(\pi r_0 - 4b) + b(1 - b/r_0)^{2\gamma}(1 - \gamma)\{12r_0^2 - (1 - 2\gamma)(3\pi br_0 + 8\gamma b^2)\}} - 1} \right]. \quad (21)$$

For $\gamma = 1$, the JNW metric reduces to the Schwarzschild metric and we obtain the deflection angle to be $\hat{\alpha}(r_0) = \pi\left(\frac{1}{\sqrt{1-4b/\pi r_0}} - 1\right)$, while for $\gamma = 2$, we get the deflection angle corresponding to the JNW wormhole

$$\hat{\alpha}(r_0) = \pi \left[\sqrt{\frac{3\pi(r_0 - b)r_0^6}{3br_0^5(r_0 - b)(\pi r_0 - 4b) - 3b(r_0 - b)^4(16b^2 + 3\pi br_0 + 4r_0^2)}} - 1 \right]. \quad (22)$$

At large distance the deflection angle in the weak field limit is given by

$$\begin{aligned} \hat{\alpha}(r_0)|_{r_0 \rightarrow \infty} &= \frac{2b\gamma}{r_0} + \frac{b^2}{2\pi r_0^2} \left[12\gamma^2 - \pi(4 - \pi)(1 - 3\gamma + 2\gamma^2) \right] \\ &+ \frac{b^3}{6\pi^2 r_0^3} \left[3\pi^3(1 - \gamma)(1 - 2\gamma)^2 + 120\gamma^3 - 72\pi\gamma(1 - 3\gamma + 2\gamma^2) \right. \\ &\left. - 2\pi^2(6 - 37\gamma + 69\gamma^2 - 38\gamma^3) \right] + O\left(\frac{1}{r_0}\right)^4 \end{aligned} \quad (23)$$

b) Ellis wormhole

The Ellis wormhole is described by the metric [9, 13, 17]

$$ds^2 = dt^2 - dr^2 - (r^2 + a^2)(d\theta^2 + \sin^2\theta d\phi^2) \quad (24)$$

and from Eq.(6) the potential function $V(z)$ is found to be

$$V(z) = \left(\frac{r_0^2 - a^2}{r_0^2 + a^2}\right) z^2 + \left(\frac{a^2}{r_0^2 + a^2}\right) z^4. \quad (25)$$

It follows from Eq.(13) that the deflection angle is given by

$$\hat{\alpha}(r_0) = \pi \left[\sqrt{\frac{2(r_0^2 + a^2)}{2r_0^2 + a^2}} - 1 \right], \quad (26)$$

and in the weak field limit it becomes

$$\hat{\alpha}(r_0)|_{r_0 \rightarrow \infty} = \frac{a^2\pi}{4r_0^2} - \frac{5a^4\pi}{32r_0^4} + \frac{13a^6\pi}{128r_0^6} - \frac{141a^8\pi}{2048r_0^8} + O\left(\frac{1}{r_0}\right)^{10}. \quad (27)$$

Eqs.(21) and (26) gives the expression of the deflection angles in the strong field which is useful to calculate various lens parameters for these wormholes.

IV. Numerical results

To explore the physical content, let us proceed to analyze the deflection angle and various lens parameters for two wormholes numerically. It is easy to see that for the JNW wormhole, the radius of the photon sphere is given by $r_{ph}^{JNW} = 4.27m$ for $\gamma = 2$ which is less than the value predicted by the photon sphere equation [5]. This result may be improved by including the higher order calculation recently developed by Amore et al [20]. Fig.1 shows the variation of the deflection angle with the closest distant of approach for the JNW wormhole. We note that the deflection angle asymptotically goes to infinity when x_0 ($= \frac{r_0}{2m}$) approaches to the photon sphere. To compare this with the Ellis wormhole, Fig.2 depicts the plot of deflection angle with closest distant of approach for this wormhole for different values of the throat parameter a . It follows that, unlike the JNW case, the deflection angle attains a critical maximum value of $\hat{\alpha}(0) = 1.30$ radian (74.6 degrees). This manifestly shows the non-existence of the photon sphere for the Ellis wormhole indicating the absence of the relativistic images for this wormhole. This result for the Ellis wormhole also follows from the photon sphere equation [5] and it contradicts with the results of Perlick [19] who argued for the existence of its relativistic images.

To calculate the separation between the leading relativistic images for a typical JNW metric we take $M = 2.8 \times 10^6 M_\odot$ and the the lens-observer distance $D_d = 8.5\text{kpc}$. Furthermore, we consider that the lens is situated at half way between the source and the observer, i.e., $D_{ds}/D_s = 1/2$ and the throat parameter to be $a = 10$ km. For different values of γ , Table-I illustrates closest approach distance x_0 , Einstein ring (θ_E) with corresponding deflection angle (α_E) and the separation between the first relativistic image (θ_1) with other relativistic images packed together (θ_∞) given by $s = \theta_\infty - \theta_1$:

Table I: Einstein ring and the relativistic images for JNW wormhole

γ	x_0, α_E (arcsec), θ_E (arcsec)	θ_1 (μ arcsec)	θ_∞ (μ arcsec)	$s = \theta_\infty - \theta_1$ (μ arcsec)
1.0	178457, 2.31166, 1.15582	16.885295	17.792393	0.907098
1.5	218564, 2.83119, 1.41558	25.921124	26.712847	0.791723
2.0	252376, 3.26919, 1.63458	34.843479	35.663729	0.820249

Finally we note that the Einstein angle for the JNW metric is given by $\theta_E^{JNW} = \sqrt{\frac{4\gamma m D_{ds}}{D_d D_s}}$ while that for the Ellis is $\theta_E^{Ellis} = (\frac{\pi a^2 D_{ds}}{4D_d^2 D_s})^{(2/3)}$. This readily shows that the ratio $\frac{\theta_E^{JNW}}{\theta_E^{Sch}} \approx 1.41$ ($\gamma = 2$) and $\frac{\theta_E^{Ellis}}{\theta_E^{Sch}} \approx 10^{-17}$, indicating that the Einstein ring of the JNW wormhole is much larger than the Ellis wormhole. Furthermore, with the throat parameter $a = 10km$, the Einstein ring of the Ellis wormhole is found to be $\theta_E^{Ellis} \approx 1.07 \times 10^{-11}$ micro-arcsecond and therefore it is too small to be visible.

To see how the qualitative features of the lens parameters of both wormholes are similar, we compare the magnification curves of the JNW wormhole ($\gamma = 2$) with that of the Ellis wormhole. Fig.3 and 4 depict the plots of the tangential magnification (μ_t) and total magnification (μ) as the function of the image position θ near the angular radius of the Einstein ring. For both wormholes the singularities in these curves give the tangential critical curves (TCC). Similarly Fig.5 and 6 show the variation of the radial magnification (μ_r) where the absence of the singularity indicates that we do not have any radial critical curve (RCC).

V. Conclusion

The search for the wormholes by studying the mirror images formed due to the gravitational lensing is one of the most intriguing way to prove the existence of the exotic matter in nature. In this paper we have explicitly calculated the deflection angle using the methodology developed by Amore and Diaz for the JNW and Ellis wormholes respectively. It is shown that the Einstein ring of the JNW wormhole is much larger in comparison to that of the Ellis wormhole. Furthermore, the JNW wormhole exhibits the relativistic images in contrast to the Ellis wormhole which does not have any photon sphere. A careful analysis

of this pattern of the images may shed some light on possible signature of the exotic lensing object which gives rise to the wormhole geometry.

Acknowledgement

TKD thanks the University Grants Commission, New Delhi and SS thanks Department of Science and Technology, New Delhi for partial support. SS thankfully acknowledges the Visiting Associateship of S N Bose National Centre for Basic Sciences, Kolkata.

References

- [1] J N Hewitt *et al*, Nature (London) **333**, 537 (1988)
- [2] J Wambsganss, "Gravitational Lensing in Astronomy", astro-ph/9812021
- [3] P Schneider, J Ehlers and E E Falco, *Gravitational Lenses* (Springer-verlag, Berlin, 1992)
- [4] K S Virbhadra and G F R Ellis, Phys Rev D **62**, 084003 (2000)
- [5] K S Virbhadra and G F R Ellis, Phys Rev D **65**, 103004 (2002)
- [6] K S Virbhadra, D Narasimha and S M Chitre, Astr & Astrophys **337**, 1 (1998)
- [7] V Bozza, Phys Rev D **66**, 103001 (2002)
- [8] M S Morris and K S Thorne, Am J Phys **56**, 395 (1988)
- [9] K K Nandi, Y Z Zhang, A V Zakharov, Phys Rev D **74**, 024020 (2006)
- [10] C Armendáriz-Picon, Phys Rev D **65**, 104010 (2002)
- [11] J G Cramer, R L Forward, M S Morris, M Visser, G Benford, G A Landis, Phys Rev D **51**, 3117 (1995)
- [12] M Visser, *Lorentzian wormholes*, AIP Press, New York 1995

- [13] S Weinberg, *Gravitation and Cosmology: principles and applications of the general theory of relativity*, John Wiley & Sons, New York 1972
- [14] P Amore and S A Diaz, Phys Rev D **73**, 083004 (2006)
- [15] S Frittelli, T P Kling and T Newman, Phys Rev D **61**, 064021 (2000)
- [16] A I Janis, E T Newman and J Winnicour, Phys Rev Lett **20**, 878 (1968)
- [17] M Wynman, Phys Rev D **24**, 839 (1981)
- [18] H G Ellis, J Math Phys, **14**, 104 (1973)
- [19] V Perlick, Phys Rev D **69**, 064017 (2004)
- [20] P Amore, S Arceo and F M Fernández, Phys Rev D **74**, 083004 (2006)

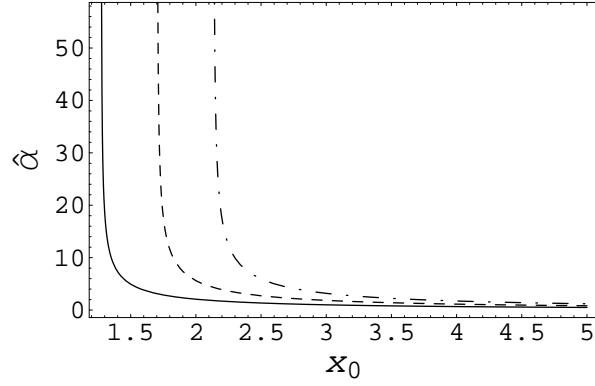


Fig.1: Variation of the deflection angle (in degree) of the JNW metric with the distance of closest approach x_0 ($x_0 = \frac{r_0}{2m}$) for $\gamma = 1$ (continuous curve), $\gamma = 1.5$ (dashed curve) and $\gamma = 2$ (dot-dashed curve).

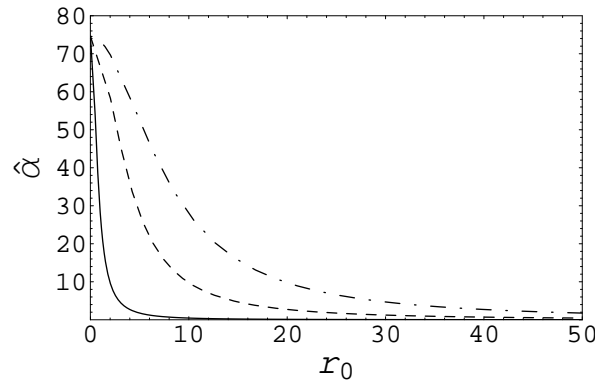


Fig.2: Variation of the deflection angle (in degree) with the distance of closest approach r_0 (in km) for the Ellis wormhole with throat parameter, $a = 1$ km (continuous line), $a = 5$ km (dashed line), $a = 10$ km (dot-dashed line).

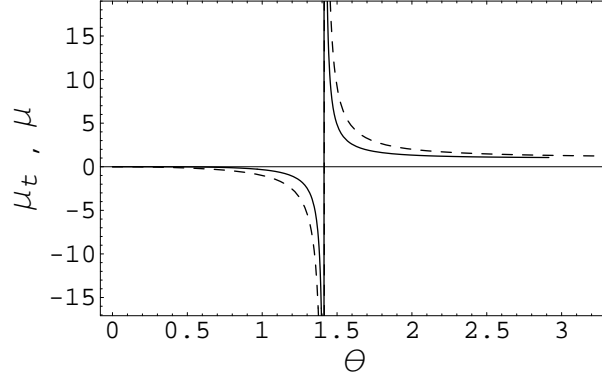


Fig.3: The tangential magnification μ_t (dashed curve) and total magnification μ (continuous curve) of the JNW wormhole with $\gamma = 2$ as the function of the image position θ (in arcsecond) near the Einstein angle.

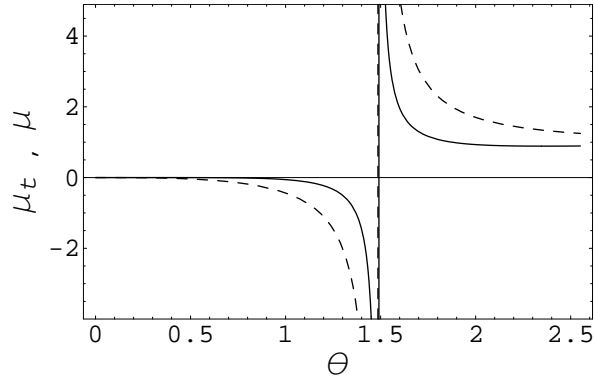


Fig.4: The tangential magnification μ_t (dashed curve) and total magnification μ (continuous curve) of the Ellis wormhole ($a = 10$ km) as the function of the image position θ (in micro-arcsecond) near the Einstein angle.

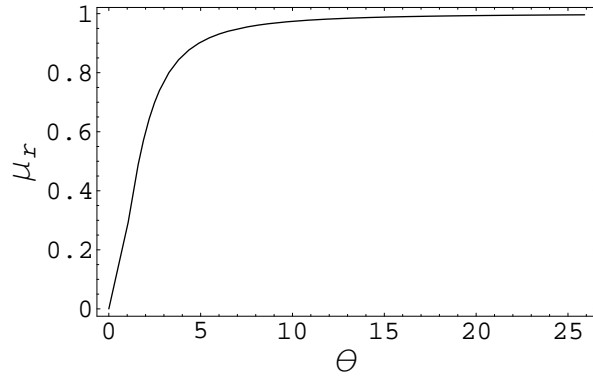


Fig.5: The radial magnification μ_r plotted against θ (in arcsecond) for the JNW wormhole with $\gamma = 2$.

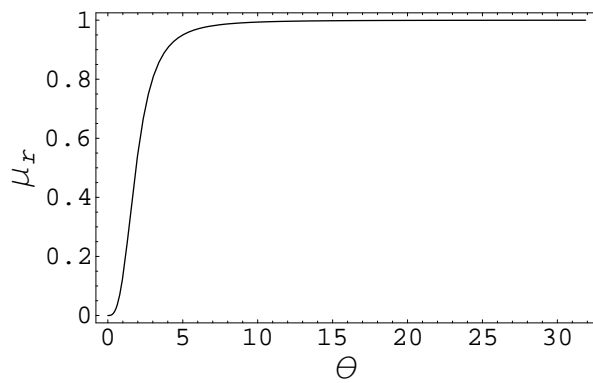


Fig.6: The radial magnification μ_r versus θ (in microarcsecond) for the Ellis wormhole ($a = 10$ km).